Article

pubs.acs.org/Biomac

Two-Step Self-Assembly of Liposome-Multidomain Peptide Nanofiber Hydrogel for Time-Controlled Release

Navindee C. Wickremasinghe,[†] Vivek A. Kumar,[†] and Jeffrey D. Hartgerink*[,†,‡]

Departments of [†]Chemistry and [‡]Bioengineering, Rice University, Bioscience Research Collaborative, 6500 Main Street, Houston, Texas 77030, United States

Supporting Information

ABSTRACT: Progress in self-assembly and supramolecular chemistry has been directed toward obtaining macromolecular assemblies with higher degrees of complexity, simulating the highly structured environment in natural systems. One approach to this type of complexity are multistep, multicomponent, self-assembling systems that allow approaches comparable to traditional multistep synthetic organic chemistry; however, only a few examples of this approach have appeared in the literature. Our previous work demonstrated nanofibrous mimics of the extracellular matrix. Here we demonstrate the ability to create a unique hydrogel, developed by stepwise self-assembly of multidomain peptide fibers and liposomes. The two-component system allows for controlled release of bioactive factors at multiple time points. The individual components of the self-assembled gel and the composite hydrogel were characterized by TEM, SEM, and rheometry, demonstrating that peptide nanofibers and lipid vesicles both retain their structural integrity in the composite gel. The rheological robustness of the hydrogel is shown to be largely unaffected by the presence of liposomes. Release studies from the composite gels loaded with different growth factors EGF, MCP-1, and PlGF-1 showed delay and prolongation of release by liposomes entrapped in the hydrogel compared to more rapid release from the hydrogel alone. This bimodal release system may have utility in systems where timed cascades of biological signals may be valuable, such as in tissue regeneration.

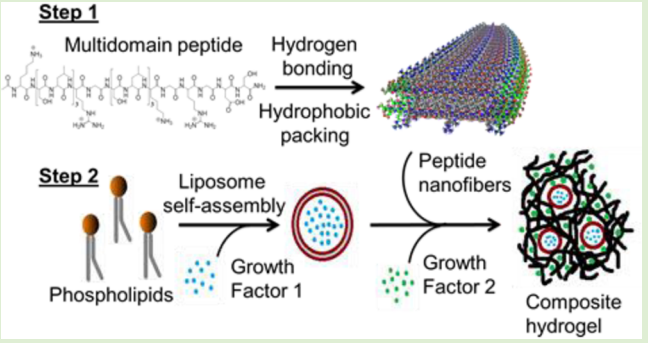

INTRODUCTION

To achieve the high level of complexity and functionality seen in the sophisticated biological systems of nature, we must develop self-assembling systems that make use of multiple components capable of displaying orthogonal self-assembly.[1] This is a process wherein two or more supramolecular assemblies form independently in a single system each with its own characteristics.[1,2] In this study we demonstrate the ability of multidomain peptides (MDPs) to self-assemble independently into a fibrous network in the presence of another supramolecular entity, liposomes. The resultant composite hydrogel is shown to exhibit favorable bimodal release characteristics when loaded with bioactive factors. This indicates the potential of the self-assembled hydrogel to display comparable functionality to the natural extracellular matrix (ECM) in terms of chemical communication by signaling molecules.

Hydrogel scaffolds provide structural integrity and potentially mimic the nanofibrous ECM while controlling drug and protein delivery to tissues.[3] The extracellular milieu presents a chemically diverse environment that provides structural support and interacts with cells, allows oxygen, nutrient and small molecule exchange in the interstices and also provides a template for wound healing. This exchange over diffusion gradients, and in some cases active transport against a gradient to build a potential can translate to regulated cell growth, proliferation, differentiation, and targeted apoptosis in response to a variety of stimuli.[4] Mimicry of structure and function of this complex environment has been a mainstay of tissue engineering endeavors. To this end, the use of engineered biomaterials, such as hydrogels formed with self-assembling peptides and liposomal carriers, to interface with biological systems and affect controlled delivery of bioactive factors is of critical importance in tissue engineering and therapeutic applications.[5]

Hydrogel preparation employing self-assembly of peptides offers facile biomimicry.[6,7] Short chain oligopeptides with ECM protein-mimicking sequences can be rapidly synthesized and allowed to self-assemble under controlled conditions to form fibrous networks which in turn entangle further to yield mechanically robust hydrogels.[8−16] MDPs consist of polar terminal residues (lysine) with alternating hydrophilic (serine) and hydrophobic (leucine) residues, as previously reported.[7,17] These hydrophobic/hydrophilic residues create facial amphi-

Received: June 11, 2014
Revised: August 18, 2014
Published: September 9, 2014

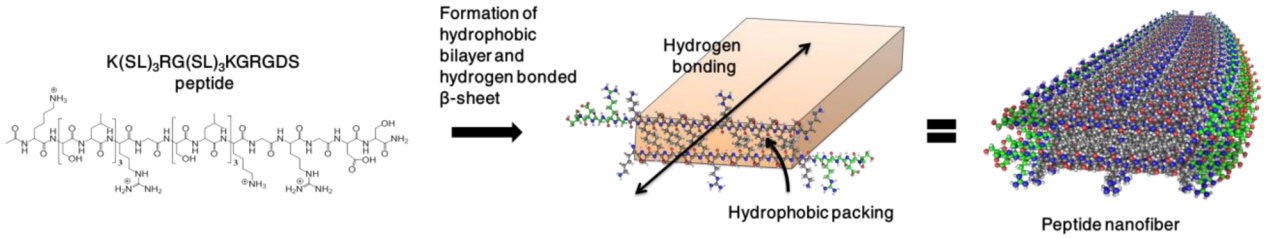

Figure 1. Schematic of the process of multidomain peptide self-assembly in to nanofibers. Multidomain peptide scaffolds with the sequence $K(SL)_3RG(SL)_3KGRGDS$ form facial amphiphiles that self-assemble into β-sheet forming fibers. With the introduction of multivalent salts, terminal charge repulsion is shielded allowing for long-range fiber growth.

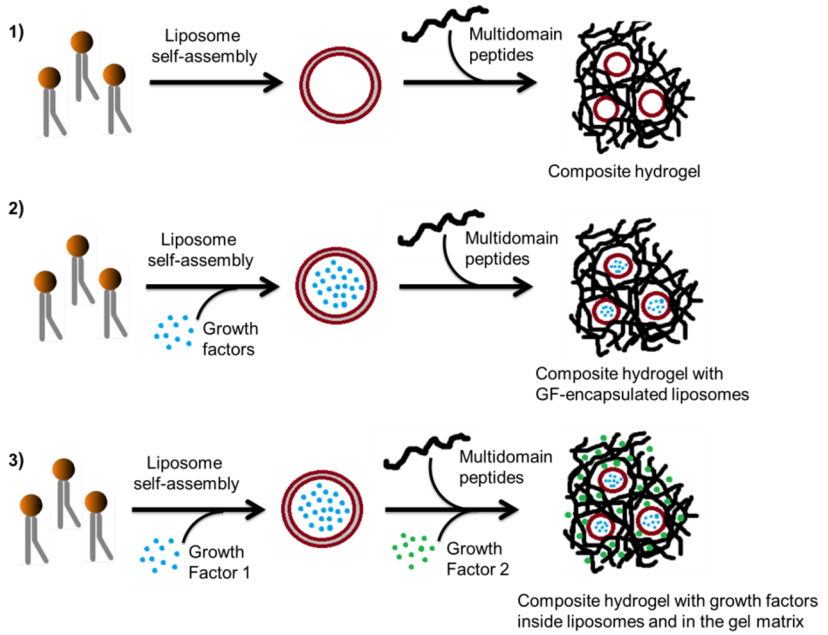

Figure 2. Stepwise orthogonal self-assembly combining liposomes, growth factors, and MDP fibers.

philes that self-assemble by eliminating water in hydrophobic regions, and form extensive hydrogen bonding networks. In the process of self-assembly, terminal residue positive charges repel lateral fiber growth,[17,18] resulting in a phenomenon termed molecular frustration. With the addition of multivalent ions in buffer systems such as PBS, terminal lysine residues are shielded, overcoming molecular frustration and allowing long-range fiber growth.[6] Physical and chemical cross-links in MDP hydrogels are formed through noncovalent cross-linking.[7] These bonds easily break and reform allowing the hydrogels to undergo shear thinning and recovery.[19] Rationally designed sequences afford the ability to tailor biological activity. In our system we have added a cell adhesion (RGD) moiety derived from fibronectin, and a central matrix metalloproteinase (MMP) cleavage sequence (LRG) to allow biodegradation (Figure 1).[17] We have demonstrated injectability,[19] biodegradability,[17] and biocompatibility[20] of these hydrogel scaffolds. For desired cellular/tissue outcomes that cannot be achieved by the peptide sequence alone, we have shown the ability to release growth factors from MDP matrices.[20]

The regeneration of functional tissues in most cases employs the approach of combining three main elements: cells, biochemical/mechanical factors, and scaffolds.[21,22] Therefore, the incorporation of bioactive factors such as growth factors (GFs) and cytokines as well as engineering their controlled release over time is critical for directing and sustaining growth, proliferation and correct differentiation of cells in the scaffold.[23] Controlled or delayed release is often preferred over immediate release of bioactive factors due to the slow, steady output and consequent availability of chemicals over longer periods of time, which leads to a prolonged host response. It is also known to enhance safety, efficacy, and reliability of drug therapy.[24,25] Controlled release from hydrogel scaffolds and other implanted materials have been demonstrated in a variety of ways in the recent past: heparin binding to tether GFs to the peptide hydrogel,[20,26] pH-responsive gel beads encapsulating protein,[24,27] drug eluting layer-by-layer polyelectrolyte film coatings on scaffolds,[28] degradable hydrogels and microspheres,[27] and liposome encapsulation of protein/drug.[29,30] The two main types of release from hydrogel scaffolds is diffusion-controlled release and degradation-controlled release.[5] Diffusion-controlled release leads to rapid release of bioactive factors from hydrogels due to mesh size (on the order of 100 nm) and tortuosity of the gel; typically the hydrodynamic diameter of the protein is on the order of 1 nm. In contrast, degradation-controlled release is relatively slower as the release of protein is dependent on the erosion of the carrier, bulk degradation, or a combination of both.[27]

In this paper we address the development of a system utilizing MDP hydrogels that can allow controlled release of desired growth factors and cytokines over multiple time scales. Preliminary studies on release kinetics of an MDP hydrogel

dx.doi.org/10.1021/bm500856c | Biomacromolecules 2014, 15, 3587−3595

have been explored by us.[20] Heparin binding was used to enhance binding of growth factors to peptide fibers of the gel matrix and achieve delayed release; a strategy only amenable to proteins with heparin affinity. The work reported herein focuses on developing an alternative delivery method capitalizing on liposomes as carriers of GF molecules which could be expanded to a broad spectrum of proteins or small molecules.

Liposomes are vesicles that self-assemble when phospholipids are dispersed in an aqueous environment. These vesicles contain an aqueous volume entirely enclosed by a bilayer membrane composed of lipid molecules.[31] Manipulation of size, composition, charge, and lamellarity[32] of liposomes allow material entrapment in both the aqueous compartment and within the membrane, promoting their use as vehicles to administer nutrients, drugs, and proteins.[33]

The GFs and cytokines tested for release were chosen based on the diversity of their sizes and the effects they bring about. Epidermal growth factor (EGF; 6.2 kDa) is a well-characterized growth factor involved in the growth, proliferation, adhesion and survival of various cell types, as well as tissue repair especially in the re-epithelialization stage of wound healing.[34,35] Placental growth factor-1 (PlGF-1; 29.7 kDa) is a key angiogenic and vasculogenic factor, particularly in embryogenesis, belonging to the vascular endothelial growth factor (VEGF) family[36−38] Monocyte chemoattractant protein-1 (MCP-1; 8.6 kDa) is a highly produced chemokine in resident and inflammatory cells of a wound site and it acts in recruiting monocytes, macrophages, and lymphocytes to sites of tissue damage.[39,40] Testing three different bioactive factors for release and obtaining similar release profiles for all three confirms the broad delivery applicability of the bimodal release system established herein.

We believe a composite nanofiber-liposome hydrogel will be a more generalized delivery strategy for bimodal controlled release, largely independent of the entrapped material.[33] The success of liposomes as GF delivery agents has been demonstrated previously by numerous studies.[33,41−43] Furthermore, liberation of liposomal contents will only occur after fusion of liposomal membranes to cell membranes, engulfment of liposomes by cells, and collapse of liposomes due to instability.[33] As such, release of GFs will be degradation-based and thus delayed significantly as compared to release from the hydrogel alone.

In this report we show the ability to achieve bimodal release of growth factors and cytokines. Specifically, we incorporate passive diffusion and liposomal delivery methods to achieve bimodal delivery of drugs (Figure 2). The MDP used, $K(SL)_3RG(SL)_3KGRGDS$, was coupled with a controlled release system utilizing liposomal encapsulation of three different GFs/cytokines labeled with a reporter molecule (EGF-FITC, MCP-1-CFDA, PlGF-1-TAMRA). The resulting hybrid gels consisting of two supramolecular assemblies exhibit: (i) composite macro-structural features, (ii) no significant change in mechanical properties, and (iii) bimodal drug release.

EXPERIMENTAL SECTION

Synthesis and Characterization of MDP. The MDP used to create hydrogels has the sequence $K(SL)_3RG(SL)_3KGRGDS$, containing a matrix metalloproteinase 2 (MMP2) sensitive cleavage site LRG and a cell adhesion site RGD.[17] Peptide was synthesized on a low loading Rink Amide MBHA resin at a 0.15 mM scale using a Focus XC automated solid phase peptide synthesizer (Aapptec, Louisville, KY) by using an optimized protocol reported previously.[7,6] Amino acids were added in a 4:1 excess to the synthesizing peptide. HATU and DiEA were used to couple amino acids to the peptide. Deprotection was achieved using 25% piperidine in a 1:1 DMF/DMSO solvent mixture. The N-terminus was deprotected and acetylated. Peptide was cleaved from the resin using a cocktail of TFA, triisopropylsilane, water, ethanedithiol and anisole in a 36:1:1:1:1 ratio. Resulting peptide had neutralized termini due to the acetylated N-terminus and amidated C-terminus. Cleaved peptide was rotoevaporated to reduce overall volume and peptide precipitated in cold ether, concentrated and dried overnight. Dried peptide was dissolved in Milli-Q water to form a 1% or 2% by weight solution and pH adjusted to 7.4 with 0.1 M NaOH. Solution was dialyzed (MWCO 500−1000 Da) for 3 days with buffer changes twice daily. Postdialysis, the peptide solution was frozen and lyophilized.

Mass spectrometry and circular dichroism: Synthesis of the correct peptide was confirmed by matrix-assisted laser desorption/ionization time-of-flight (Bruker Daltonics, Billerica, MA) mass spectroscopy. (MALDI-TOF) Secondary structure of the peptide was evaluated employing circular dichroism (CD). CD data was collected on a Jasco J-810 spectropolarimeter (Jasco, Tokyo, Japan). The peptide was dissolved in Milli-Q water to make a 0.01% by weight solution at neutral pH. Data was collected at room temperature from 180 to 250 nm using a 0.01 cm quartz cuvette. Molar residual elipticity ($[\theta]$) was calculated from milidegrees (θ) using path length (l) in cm, molecular weight (M) in grams per mole, peptide concentration (c) in mg/mL, and number of residues (n_r).

$$[\theta] = \frac{\theta \times M}{c \times l \times n_r \times 10}$$

Negatively Stained TEM. MDP nanofiber formation has been demonstrated by negatively stained transmission electron microscope (TEM) images of 1% by weight peptide samples made in 298 mM sucrose. A 2% by weight solution of phosphotungstic acid (PTA) was prepared at pH 7 and syringe filtered through a 0.2 μm filter before use as the negative stain. Two drops of bacitracin (0.1 mg/mL) was pipetted onto a Quantifoil R1.2/1.3 holey carbon mesh copper grid and allowed to sit for 3 min. Bacitracin was used as a wetting agent to increase spreading of sample on grid. Excess solution was wicked away with filter paper. A total of 10 μL of peptide sample was pipetted on to grid and allowed to sit for 10 min. The excess was blotted away and finally a drop of PTA stain was added on to grid and allowed to sit for another 3 min. Excess stain was wicked away and grid was kept to dry overnight before TEM imaging. All imaging was performed using a 80.0 kV JEOL 1230 high contrast transmission electron microscope (JEOL USA Inc., Peabody, MA).

Synthesis and Characterization of Liposomes. Phospholipids and cholesterol were purchased from Avanti Polar Lipids, Inc. Dipalmitoylphosphatidylcholine (DPPC), Dipalmitoylphosphatidylglycerol (DPPG) and cholesterol were mixed in chloroform in the molar ratio 5:1:4 and solvent evaporated by passing a gentle stream of nitrogen.[33] The dried lipids were left under high vacuum overnight to allow complete evaporation of chloroform. Dry lipid films were hydrated with 1× phosphate-buffered saline (PBS). The mixture was sonicated briefly and incubated for 1 h with intermittent agitation. Then it was subjected to five freeze−thaw cycles (rapidly frozen in a dry ice−butanol bath and thawed in a water bath at 41 °C). The liposome suspension was extruded through a 100 nm polycarbonate membrane using a Mini-Extruder (Avanti Polar Lipids Inc., Alabaster, AL).

Dynamic light scattering: Liposomes were sized by dynamic light scattering experiments performed on a Malvern Zen 3600 Zetasizer (Malvern Instruments Ltd., Malvern, U.K.). The purified liposome suspension was added to a low volume disposable cuvette up to a maximum height of 10 mm and data was collected at room temperature. The refractive index of PBS was entered as 1.33, viscosity as 1.05 cP at room temperature, and dielectric constant as 78.3. Absorbance of liposome suspension was measured and input as 0.1. Liposomes were incubated at 37 °C for 14 days and sized again to evaluate their stability.

Cryogenic TEM. Vitreous ice TEM samples of liposomes were prepared for imaging. First, the TEM grids were ionized by glow discharging for 1 min with a 5 mA discharge. The next stages of sample preparation were all performed using a Vitrobot type FP5350/60. The liposome suspension or nanofiber solution was added to the grid and immediately blotted for 2 s in a humidity-controlled chamber before being immersed in liquid ethane. The grid is then manually transferred from the liquid ethane to liquid nitrogen where it is stored until imaging. All TEM imaging was performed on a 200 kV JEM 2010 transmission electron microscope (JEOL USA Inc., Peabody, MA) and cryo-imaging was taken at a temperature of −176 °C using minimum dose system (MDS) mode.

Formation and Characterization of Composite Hydrogel. The lyophilized peptides were dissolved at 20 mg/mL in Milli-Q water with 298 mM sucrose, and the pH was adjusted to 7.4. Composite gels were prepared by mixing 20 mg/mL peptide solution with the liposome suspension in a 1:1 ratio, while control gels were made with 1× PBS only instead of with liposomes in PBS, for a final concentration of 1% by weight in both cases. The composite gel was imaged by negatively stained TEM, cryogenic-TEM, and scanning electron microscopy (SEM). All TEM samples of the composite gel were prepared as mentioned previously for the peptide fibers and liposomes.

Scanning Electron Microscopy. Gels were fixed in formalin overnight and dehydrated in a series of ethanol/water solutions progressing from 30% ethanol to 100% ethanol over the course of 24 h. The dehydrated gels were critical point dried for 1 h using an EMS 850 critical point drier (Electron Microscopy Sciences, Hatfield, PA). They were affixed to SEM stubs using conductive carbon tape. Samples were sputter coated with 8 nm gold using a Denton Desk V Sputter System (Denton Vacuum LLC USA, Moorestown, NJ) and imaged using a JEOL 6500F scanning electron microscope at 15.0 kV (JEOL USA Inc., Peabody, MA).

Rheology. The rheological properties of the MDP gel and composite gel were tested using oscillatory rheology. All rheological studies were performed on a TA Instruments AR-G2 rheometer (TA Instruments, New Castle, DE). A total of 100 μL of prepared hydrogel was deposited onto the rheometer stage. A 12 mm stainless steel parallel plate was used with a 250 μm gap height. Strain sweep experiments were performed at a frequency of 1 rad/s (which was determined to be in the linear viscoelastic region) from 0.001 to 100% strain. Shear recovery experiments were carried out by subjecting the gel to 0.5% strain for 10 min, increasing the strain to 100% for 1 min, then reducing the strain back to 0.5% for 15 min.

Growth Factor Conjugation to Fluorophore Molecules. Epidermal growth factor conjugated to fluorescein isothiocyanate (EGF-FITC) was purchased from Life Technologies. Monocyte chemotactic protein-1 (MCP-1) and placental growth factor-1 (PlGF-1) were purchased from PeproTech Inc., (Rocky Hill, NJ) and conjugated to 5(6)-carboxyfluorescein diacetate succinimidyl ester (CFDA-SE) and 5(6)-carboxytetramethyrhodamine succinimidyl ester (TAMRA-SE), respectively, using standard labeling protocols. A total of 9 mM CFDA-SE in sterile anhydrous DMSO was mixed with 0.2 mM MCP-1 in PBS in a molar ratio of 20:1, while 9 mM TAMRA-SE in sterile anhydrous DMSO was mixed with 0.07 mM PlGF-1 in PBS in a molar ratio of 5:1. Both mixtures (total volume = 20 μL in each case) were incubated overnight in the dark at 4 °C with continuous gentle agitation. The unconjugated dye was removed from the conjugated protein by using SpinOut GT-600 0.1 mL columns (G-Biosciences, St. Louis, MO), and the conjugated protein was eluted out with PBS.

Loading Liposomes with Growth Factors. Encapsulation of labeled GFs was carried out in situ during the hydration phase of liposome preparation. A solution of labeled GF in 1× PBS supplemented with 0.1% bovine serum albumin (BSA) was used to hydrate the dry lipid films. Incubation, freeze−thaw cycles, and extrusion of the liposomes with labeled GF were carried out as previously mentioned. After extrusion, the unencapsulated GF was removed by passing the liposome suspension through a Sephadex G-50 column (G-75 in the case of PlGF-1-TAMRA). The purified GF-loaded liposomes were sized by DLS and utilized to form composite hydrogels. Efficiency of encapsulating GF was determined by quantifying the amount of labeled GF removed via Sephadex column, m_1, compared to the concentration of GF in the original hydration solution, m_2 ($100 \times (m_2 - m_1)/m_2$).

All experiments with labeled GF were done in the dark with containers covered in aluminum foil to protect the fluorescent molecules from light. Fluorescence was measured using a Tecan Infinite M1000 plate reader (Tecan Systems Inc., San Jose, CA).

GF Release from Composite Gel. GF release from liposomes in the composite gel was assayed over time utilizing a transwell set up (Figure 3). Composite gels were made in triplicate and topped with

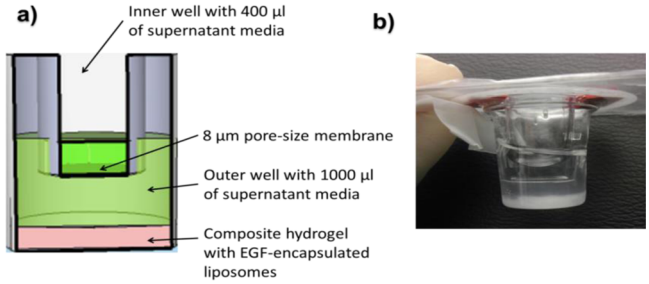

Figure 3. (a) Schematic diagram and (b) photograph of a transwell set up for EGF-FITC release studies.

supernatant media consisting of PBS supplemented with 0.1% BSA. The inner well of the transwell construct also contained supernatant media able to flow freely across an 8 μm pore size membrane in order to achieve a uniform concentration of media throughout both wells. Gels were incubated at 37 °C and 5% CO_2 for at least 14 days (18 days in the case of EGF-FITC). 100 μL of the release media was removed from the inner well and replenished with fresh media at a series of time points (days 1, 3, 7, 11, 14, 18). Amount of labeled GF released from the composite gel at each time point was quantified by measuring fluorescence and relating it to concentration of labeled GF through a standard curve (a sample standard curve is given in Supporting Information, Figure S2). A separate series of standards were prepared for each time point at the beginning of the release study and incubated along with the transwell constructs as internal references.

RESULTS

Synthesis and Characterization of MDP Fibers and Liposomes. Successful synthesis and purification of K-$(SL)_3$RG$(SL)_3$KGRGDS was confirmed by conducting mass spectrometry on the lyophilized peptide. β-sheet formation by the MDP was evaluated by circular dichroism (CD). In the CD spectrum, a maximum is observed near 195 nm and a minimum near 216 nm, both of which correlate with β-sheet formation (MS and CD spectra obtained are given in Supporting Information, Figure S1).[6,7,18] Previous studies have noted the ability for polyvalent anions to shield terminal lysine residues, overcoming molecular frustration.[6] These shielded charges allow for supramolecular assembly into large-scale microfibrils in water, sucrose, and other physiologically relevant buffer solutions, as we have previously demonstrated.[7,17,20] Further, MDP nanofiber formation has been demonstrated by negatively stained TEM images of 1% by weight peptide samples made in 298 mM sucrose (Figure 4a).

Liposomes were prepared by the well-known method of hydration of dry lipid films using phosphate-buffered saline as the hydration buffer.[33,44] Liposome suspension was sized by extrusion through a 100 nm pore-size filter in order to obtain a population of small unilamellar vesicles (SUVs).[45,46] Size distribution in the bulk SUV solution recorded by DLS showed

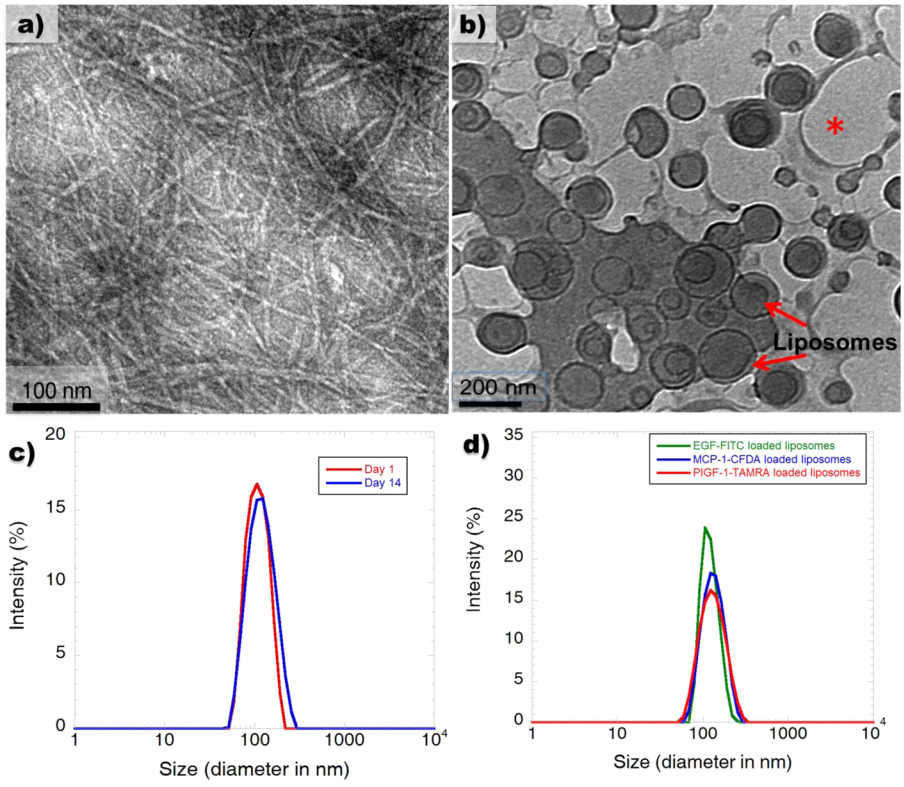

Figure 4. (a) Negatively stained TEM of 1 wt % K(SL)3RG(SL)3KGRGDS peptide in 298 mM sucrose, (b) cryo-TEM of GF-encapsulated liposomes (indicated by red arrow) and drying artifacts (indicated by *), and dynamic light scattering showing (c) size plot of unloaded liposomes showing stability over 14 days and (d) size plot of EGF-FITC, MCP-1-CFDA, and PlGF-1-TAMRA loaded liposomes after purification.

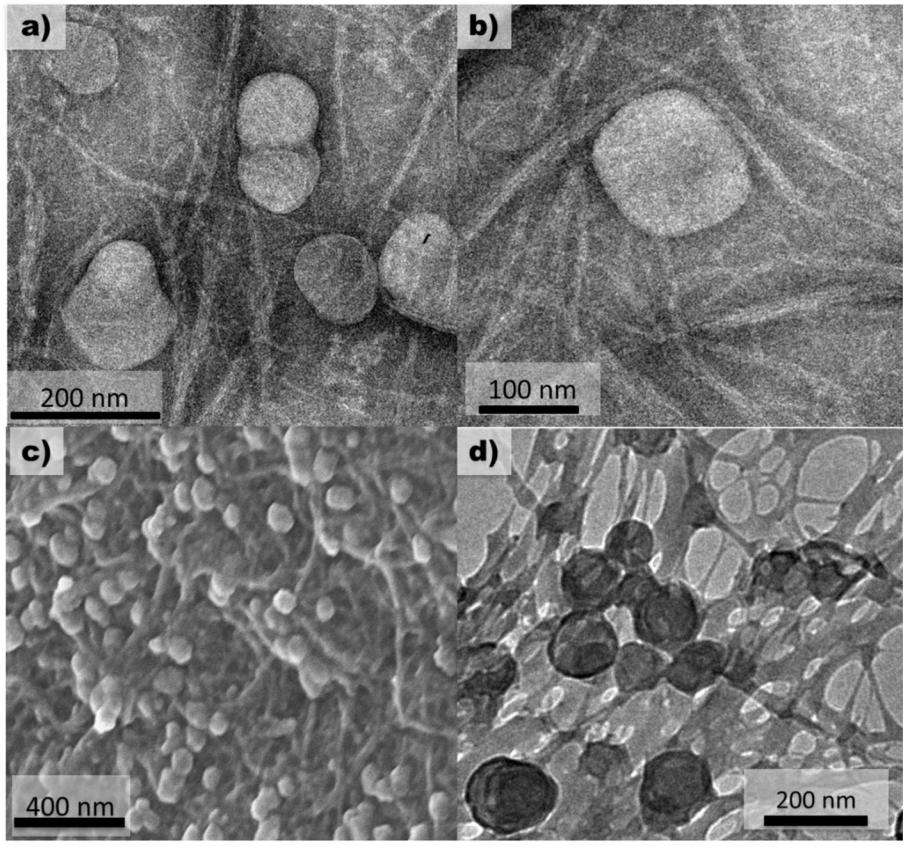

Figure 5. (a, b) Negatively stained TEM images of composite gel. (c) SEM image and (d) Cryo-TEM image of composite gel.

dx.doi.org/10.1021/bm500856c | *Biomacromolecules* 2014, 15, 3587−3595

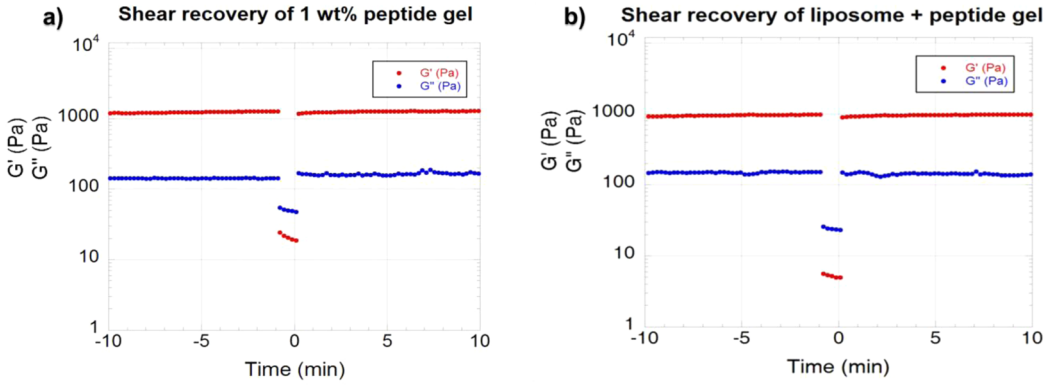

Figure 6. Shear recovery of gel without liposomes (a) compared to the composite gel with liposomes (b).

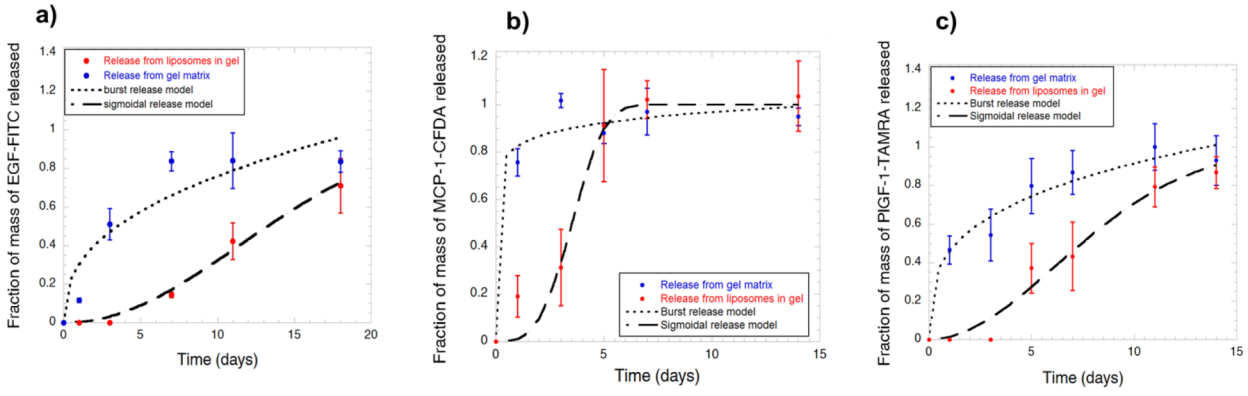

Figure 7. Release profiles for (a) EGF-FITC, (b) MCP-1-CFDA, and (c) PlGF-1-TAMRA, showing release from gel matrix of control gels without liposomes (blue) and release from liposomes in composite gels (red), along with the respective curve fit (n = 3 for each sample). R^2 values are given in SI, Table S1.

a single population of spherical particles with majority having a diameter of approximately 100 nm (±50 nm). Liposomes showed little change in size over a 14-day period, proving stability for at least up to 2 weeks at 37 °C (Figure 4c). Morphology of individual liposomes was observed via cryogenic TEM imaging (Figure 4b).

Characterization of Composite Hydrogel. MDP hydrogels containing liposomes were prepared by mixing a 2% by weight peptide solution with the liposome suspension in 1× PBS in a volume ratio of 1:1. The liposomes were prepared in a solution of PBS in order to trigger gelation of the MDP fibers to a hydrogel, once the liposomes are mixed with the peptide fibers. Presence of PBS in the liposome suspension causes elimination of electrostatic repulsion (occurring due to the lysine side chains at the termini of the MDPs) leading to physical cross-linking between fibers, which in turn allows for fiber lengthening, entanglement, and ultimately gelation, yielding a mechanically robust hydrogel.[6]

The gels were imaged by negatively stained TEM, cryo-TEM, and SEM. The stained TEM images show roughly circular liposomes with a membrane structure visible surrounded and held in place by fibers (Figure 5a,b). The cryo-TEM images also support the above representation, showing presence of clear circular structures among a network of seemingly amorphous peptide (Figure 5d). The SEM images depict the presence of spherical particles with diameters in the range of 100−200 nm, identified as liposomes, lying in a matrix of a fibrous peptide network (Figure 5c).

To evaluate the rheological properties of the composite gel, the storage modulus (G'), loss modulus (G''), and shear recovery capability of the gel were characterized using oscillatory rheology. G' was found to be ∼990 Pa compared to a storage modulus of 1200 Pa recorded for the normal hydrogel without liposomes. Shear recovery experiments demonstrated that when a shearing event is applied to breakdown the gel, its G' returns to preshear values within 1 min, indicating that the hydrogel is able to recover from shear stress (Figure 6).

Release of Labeled GFs from Liposomes in Composite Gels. During the purification of the EGF-FITC-loaded liposomes, the unencapsulated EGF-FITC was removed by passing the liposome suspension twice through a Sephadex G-50 column. Mass of the unencapsulated EGF-FITC fraction collected from the column was found by measuring fluorescence and relating it to the corresponding concentration of EGF-FITC using a standard curve. By comparing above mass with that of the original EGF-FITC quantity added during liposome preparation, efficiency of encapsulation was calculated as 67% (Supporting Information, Figure S2b). Similarly, efficiencies of encapsulation of MCP-1-CFDA and PlGF-1-TAMRA were determined as 80 and 62%, respectively. DLS experiments indicated that size distribution of the GF-loaded liposomes, after extrusion and purification, was similar to the distribution observed for unloaded liposomes (Figure 4d).

Composite gels consisting of labeled-GF-loaded liposomes were successfully formed in a transwell setup as shown in Figure 3 for release studies. The release profiles of EGF-FITC,

dx.doi.org/10.1021/bm500856c | Biomacromolecules 2014, 15, 3587−3595

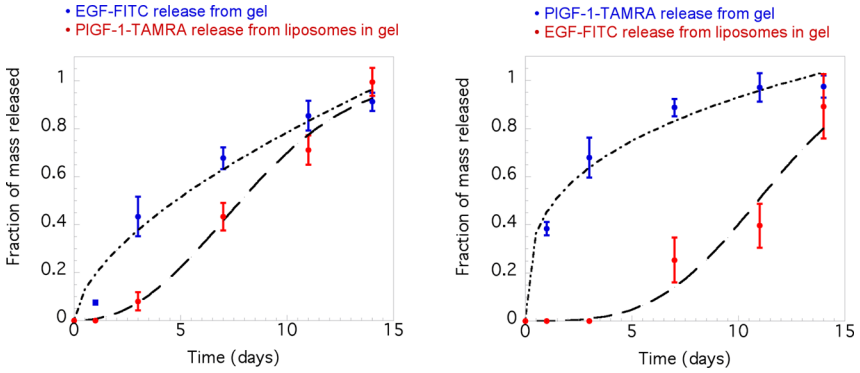

Figure 8. Release profiles obtained from the bimodal release of EGF-FITC and PlGF-1-TAMRA. Blue indicates release from hydrogel alone while red is release from liposomes within the hydrogel. Dashed lines indicate burst release or sigmoidal release models. R^2 values are given in SI, Table S2 (n = 3 for each sample).

MCP-1-CFDA, and PlGF-1-TAMRA in above composite gels and control gels without liposomes are depicted in Figure 7, which presents the time course of the total cumulative release of each of the labeled GFs. Figure 7 illustrates the ability of liposomes to delay the release of GF in to the supernatant media by approximately 5 days, compared to the control gels in which GF molecules are incorporated directly in to the hydrogel matrix without a carrier.

As seen in Figure 7a, about 80% of the EGF-FITC was released by day 7 from control gels, whereas in the composite gels, only about 15% was released at that time point and it took up to 18 days for 70% of the loaded EGF-FITC to be released. Figure 7b shows that MCP-1-CFDA molecules are rapidly released from the gel matrix so that close to 80% of the material is available in the supernatant media after 24 h of seeding the gels. However, when MCP-1-CFDA is encapsulated in liposomes within the gel, it takes up to 5 days for the same amount of material to be discharged. In the case of PlGF-1-TAMRA, we observed that the 4−5 day delay in release, relating to composite gels with liposomes, was maintained up to 2 weeks (Figure 7c). Similarity of the results pertaining to release of three different growth factor/cytokine molecules from the composite gels suggests that this controlled release system can be used with a broad variety of different bioactive factors.

The release data were modeled using two well-known functions: the Korsmeyer-Peppas equation for burst release[47,48] (eq 1) and the Weibull equation for delayed release (eq 2).[49,50]

$$\frac{M_t}{M_\infty} = k(t^n) \tag{1}$$

where M_t/M_∞ is the fraction of drug released at time t, k is the rate constant and n is the release exponent.[51]

$$\frac{M_t}{M_\infty} = 1 - e^{[-\propto(t^\beta)]} \tag{2}$$

where M_t/M_∞ is the fraction of drug released at time t, α is the scale factor corresponding to the apparent rate constant, and β is the shape factor. Using the curve fitting approach we were able to compare the differences in the nature of release between the three bioactive factors. The fit data for each case of release is given in the Supporting Information (Table S1). It is likely that EGF and PlGF-1 show some interaction with the gel matrix as they are being diffused out. Even in the case of using liposomes to delay release, EGF and PlGF-1 show slower diffusion out of the gel matrix after being released from the liposome carriers, in comparison to MCP-1, which is released relatively rapidly with and without liposomes. The faster release of MCP-1, which gives rise to a very low value for the release exponent, n, in the Korsmeyer-Peppas function and a relatively higher β value in the Weibull function, indicates that MCP-1 has minimal interaction with the gel matrix and demonstrates Fickian diffusion. In contrast, release of both EGF and PlGF-1 generate n values closer to 0.45, above which is the typical range for non-Fickian diffusion in the Korsmeyer-Peppas function.[47,51] This indicates that EGF and PlGF-1 release may be affected by interactions with the fibrous network or other factors such as polymer erosion.[48]

EGF-FITC and PlGF-1-TAMRA were incorporated into the composite gel simultaneously to demonstrate bimodal release. In the first system (Figure 8a), EGF-FITC was added to the gel matrix alone while PlGF-1-TAMRA was added to liposomes when constructing the composite gel. The reverse of this set up was tested in the second system of bimodal release (Figure 8b). Bimodal release can be achieved with two different bioactive factors added during the orthogonal self-assembly process of the composite gel. The release kinetics of one GF does not seem to be substantially affected by the presence of the other GF. The modeling studies suggest that the two tested GFs do not show any significant interactions with each other.

DISCUSSION

This study focuses on creating a complex architecture, involving two independent supramolecular assemblies, that is capable of functionally and structurally mimicking the natural extracellular matrix to a significant extent. The composite is made from GF-loaded liposomes embedded in a hydrogel matrix made of self-assembling peptides. The assembly of peptides into a nanofibrous network was hypothesized to occur independently in the presence of liposomes, which by themselves are supramolecular structures. The work reported herein elucidates the nature of such a multicomponent assembly and verifies the above hypothesis. Although there have been many studies done to elaborate, separately, the use of liposomes (in simulating biological membranes,[52,53] material capture, and release[33,54,43,42]) and fibrous networks (in representing an ECM-like environment[15,9,12]), so far only a few studies exist that combine both aspects of assembly.[1,2] From a structural point of view, this study was aimed at developing such an architecture with an apparent higher degree of complexity, which in turn will be more relevant biologically, as it may lead

dx.doi.org/10.1021/bm500856c | Biomacromolecules 2014, 15, 3587−3595

to achieving the functional complexity seen in natural systems, that is, the ECM, in terms of facilitating external communication via chemical signaling. The example particularly demonstrated is the design of a system for controlled release of bioactive factors from this architecture, which would have great potential in the field of tissue engineering and regenerative medicine.

The successful creation of a composite hydrogel using MDP fibers and labeled GF loaded liposomes, as determined by electron microscopy and rheology, has proven that orthogonal self-assembly of multiple components within a single system is a competent approach toward formation of novel and more complex architectures able to mimic naturally existing ones. Imaging by negatively stained TEM, cryogenic-TEM, and SEM revealed the nanostructural properties of the composite gel and validated the hypothesis that MDP fibers can self-assemble to a hydrogel even in the presence of liposomes and both systems can coexist in a compatible manner. Oscillatory rheology experiments showed that the mechanical integrity and robustness of the hydrogel were not destroyed by the presence of liposomes but, in fact, remained largely unaffected. Shear recovery experiments demonstrated that the composite gel is able to recover from shear stress, as has been demonstrated for MDP systems previously.[17,19] This result, combined with the high G' of the gel and general hydrogel handling properties make the composite gels with liposomes suitable for injectable tissue engineering applications. Thus, not only are the two self-assembling materials able to coexist in the presence of one another, but the assemblies are largely orthogonal as neither shape/size nor rheological properties are significantly altered.

To investigate the release kinetics of physiologically important molecules from the composite hydrogel, we chose two different growth factors and one cytokine: EGF, PlGF-1, and MCP-1 respectively, as example molecules conjugated to a fluorophore (either FITC, CFDA, or TAMRA) for detection purposes.[55,56]

The obtained release profiles of each of the labeled GFs from the composite gel demonstrate that encapsulating GFs in biocompatible carriers such as liposomes will significantly reduce the rate at which the molecules are released to the medium, thus, establishing the role of liposomes as efficacious agents for controlled release of bioactive molecules. The more or less comparable nature of all the GF/cytokine release profiles suggests the applicability of this release system to a broad range of bioactive factors and possibly even small drug molecules. Furthermore, release studies have shown that bioactive molecules can be delivered from the unique degradable composite hydrogel scaffold in two modes: (1) the early release mode, where incorporation directly in to the gel matrix allows delivery of molecules within the first 2−3 days, and (2) the late release mode, where encapsulation in liposomes allows slower, delayed delivery of molecules. This bimodal release system can be directed toward enhancing regenerative processes associated with, for example, wound healing. The process of wound healing occurs in two main stages: (1) the early stage consisting of hemostasis and inflammation, and (2) the late stage consisting of proliferation, angiogenesis, production of ECM proteins and remodeling of the ECM.[39] Each of these stages is facilitated by the release of a variety of different growth factors and cytokines such as EGF, VEGF, PlGF-1, FGF-2, MCP-1, and so on. Thus, future studies based on the bimodal release system we have constructed with the composite gel will be geared toward in vivo delivery of a combination of growth factors targeted for the early and late stages in a wound healing animal model. Additional future work will be aimed at developing multimodal release systems derived from the present work.

CONCLUSION

While both liposome self-assembly and peptide nanofiber self-assembly are governed by the same types of noncovalent interactions such as hydrogen bonding, electrostatic attraction and repulsion, and the hydrophobic effect, we have shown that their assembly is orthogonal to one another. This allows the preparation of a composite hydrogel formed from the entanglement of peptide fibers and containing spherical liposomes in a simple two-step process. The result is a construct with a higher level of structural complexity (a fibrous mesh with embedded spheres) and functionality (multimodal delivery). This has the potential of harnessing the best aspects of both materials, as the peptides can provide hydrogelation and presentation of biologically relevant signals, such as the RGD adhesion sequence, as well as enzyme-mediated degradation. Liposomes allow a more flexible loading and controlled release of proteins and which may be expanded to small molecule delivery in the future. Together growth factor-loaded liposome hydrogel can be employed as a bimodal release system aimed at delivering bioactive factors in a temporally controlled manner to enhance regenerative processes where proteins entrapped solely in the hydrogel are released quickly while those inside the liposomes are released more slowly.

ASSOCIATED CONTENT

Supporting Information

MS and CD data for the $K(SL)_3RG(SL)_3KGRGDS$ peptide, standard curves for EGF-FITC, MCP-1-CFDA, and PlGF-1-TAMRA, and additional modeling data are available. This material is available free of charge via the Internet at http://pubs.acs.org.

AUTHOR INFORMATION

Corresponding Author

*Tel.: (713) 348-4142. E-mail: jdh@rice.edu.

Notes

The authors declare no competing financial interest.

ACKNOWLEDGMENTS

The authors would like to thank Christopher Pennington, Wenhua Guo and the Shared Equipment Authority (SEA) of Rice University. The work presented in this manuscript was supported by grants from the NIH (R01 DE021798), and the Robert A. Welch Foundation (Grant No. C1557). V.A.K. gratefully acknowledges his support through an NIH F32 award (F32 DE023696).

REFERENCES

(1) Brizard, A. M.; van Esch, J. H. *Soft Matter* **2009**, *5*, 1320−1327.
(2) Brizard, A.; Stuart, M.; van Bommel, K.; Friggeri, A.; de Jong, M.; van Esch, J. *Angew. Chem., Int. Ed.* **2008**, *47*, 2063−2066.
(3) Slaughter, B. V.; Khurshid, S. S.; Fisher, O. Z.; Khademhosseini, A.; Peppas, N. A. *Adv. Mater.* **2009**, *21*, 3307−3329.
(4) Lee, K. Y.; Mooney, D. J. *Chem. Rev.* **2001**, *101*, 1869−1880.
(5) Peppas, N. A.; Hilt, J. Z.; Khademhosseini, A.; Langer, R. *Adv. Mater.* **2006**, *18*, 1345−1360.
(6) Dong, H.; Paramonov, S. E.; Aulisa, L.; Bakota, E. L.; Hartgerink, J. D. *J. Am. Chem. Soc.* **2007**, *129*, 12468−12472.

(7) Aulisa, L.; Dong, H.; Hartgerink, J. D. *Biomacromolecules* **2009**, *10*, 2694−2698.
(8) Hartgerink, J. D.; Beniash, E.; Stupp, S. I. *Science* **2001**, *294*, 1684−1688.
(9) Schneider, J. P.; Pochan, D. J.; Ozbas, B.; Rajagopal, K.; Pakstis, L.; Kretsinger, J. *J. Am. Chem. Soc.* **2002**, *124*, 15030−15037.
(10) Pochan, D. J.; Schneider, J. P.; Kretsinger, J.; Ozbas, B.; Rajagopal, K.; Haines, L. *J. Am. Chem. Soc.* **2003**, *125*, 11802−11803.
(11) Nagarkar, R. P.; Hule, R. A.; Pochan, D. J.; Schneider, J. P. *J. Am. Chem. Soc.* **2008**, *130*, 4466−4474.
(12) Jung, J. P.; Nagaraj, A. K.; Fox, E. K.; Rudra, J. S.; Devgun, J. M.; Collier, J. H. *Biomaterials* **2009**, *30*, 2400−2410.
(13) Kisiday, J.; Jin, M.; Kurz, B.; Hung, H.; Semino, C.; Zhang, S.; Grodzinsky, A. J. *Proc. Natl. Acad. Sci. U.S.A.* **2002**, *99*, 9996−10001.
(14) Holmes, T. C.; de Lacalle, S.; Su, X.; Liu, G.; Rich, A.; Zhang, S. *Proc. Natl. Acad. Sci. U.S.A.* **2000**, *97*, 6728−6733.
(15) Haines-Butterick, L.; Rajagopal, K.; Branco, M.; Salick, D.; Rughani, R.; Pilarz, M.; Lamm, M. S.; Pochan, D. J.; Schneider, J. P. *Proc. Natl. Acad. Sci. U.S.A.* **2007**, *104*, 7791−7796.
(16) Zhao, X.; Zhang, S. *Chem. Soc. Rev.* **2006**, *35*, 1105−1110.
(17) Galler, K. M.; Aulisa, L.; Regan, K. R.; D'Souza, R. N.; Hartgerink, J. D. *J. Am. Chem. Soc.* **2010**, *132*, 3217−3223.
(18) Bakota, E. L.; Sensoy, O.; Ozgur, B.; Sayar, M.; Hartgerink, J. D. *Biomacromolecules* **2013**, *14*, 1370−1378.
(19) Bakota, E. L.; Wang, Y.; Danesh, F. R.; Hartgerink, J. D. *Biomacromolecules* **2011**, *12*, 1651−1657.
(20) Galler, K. M.; Hartgerink, J. D.; Cavender, A. C.; Schmalz, G.; D'Souza, R. N. *Tissue Eng., Part A* **2012**, *18*, 176−184.
(21) Chung, C.; Burdick, J. A. *Adv. Drug Delivery Rev.* **2008**, *60*, 243−262.
(22) Nerem, R. M.; Sambanis, A. *Tissue Eng.* **1995**, *1*, 3−13.
(23) Richardson, T. P.; Peters, M. C.; Ennett, A. B.; Mooney, D. J. *Nat. Biotechnol.* **2001**, *19*, 1029−1034.
(24) El-Sherbiny, I. M.; Abdel-Bary, E. M.; Harding, D. R. K. *J. Appl. Polym. Sci.* **2010**, *115*, 2828−2837.
(25) Lin, C.-C.; Boyer, P. D.; Aimetti, A. A.; Anseth, K. S. *J. Controlled Release* **2010**, *142*, 384−391.
(26) Cai, S.; Liu, Y.; Zheng Shu, X.; Prestwich, G. D. *Biomaterials* **2005**, *26*, 6054−6067.
(27) Franssen, O.; Vandervennet, L.; Roders, P.; Hennink, W. E. *J. Controlled Release* **1999**, *60*, 211−221.
(28) Macdonald, M. L.; Samuel, R. E.; Shah, N. J.; Padera, R. F.; Beben, Y. M.; Hammond, P. T. *Biomaterials* **2011**, *32*, 1446−1453.
(29) Ruel-Gariépy, E.; Leclair, G.; Hildgen, P.; Gupta, A.; Leroux, J.-C. *J. Controlled Release* **2002**, *82*, 373−383.
(30) Nie, S.; Hsiao, W. L. W.; Pan, W.; Yang, Z. *Int. J. Nanomed.* **2011**, *6*, 151−166.
(31) Vemuri, S.; Rhodes, C. *Pharm. Acta Helv.* **1995**, *70*, 95−111.
(32) Szoka, F.; Papahadjopoulos, D. *Annu. Rev. Biophys. Bioeng.* **1980**, *9*, 467−508.
(33) Samad, A.; Sultana, Y.; Aqil, M. *Curr. Drug Delivery* **2007**, *4*, 297−305.
(34) Schultz, G.; Rotatori, D. S.; Clark, W. *J. Cell. Biochem.* **1991**, *45*, 346−352.
(35) Fan, V. H.; Tamama, K.; Au, A.; Littrell, R.; Richardson, L. B.; Wright, J. W.; Wells, A.; Griffith, L. G. *Stem Cells* **2007**, *25*, 1241−1251.
(36) Luttun, A.; Tjwa, M.; Carmeliet, P. *Ann. N.Y. Acad. Sci.* **2002**, *979*, 80−93.
(37) Carmeliet, P.; Moons, L.; Luttun, A.; Vincenti, V.; Compernolle, V.; De Mol, M.; Wu, Y.; Bono, F.; Devy, L.; Beck, H.; Scholz, D.; Acker, T.; DiPalma, T.; Dewerchin, M.; Noel, A.; Stalmans, I.; Barra, A.; Blacher, S.; VandenDriessche, T.; Ponten, A.; Eriksson, U.; Plate, K. H.; Foidart, J. M.; Schaper, W.; Charnock-Jones, D. S.; Hicklin, D. J.; Herbert, J. M.; Collen, D.; Persico, M. G. *Nat. Med.* **2001**, *7*, 575−583.
(38) Luttun, A.; Tjwa, M.; Moons, L.; Wu, Y.; Angelillo-Scherrer, A.; Liao, F.; Nagy, J. A.; Hooper, A.; Priller, J.; De Klerck, B.; Compernolle, V.; Daci, E.; Bohlen, P.; Dewerchin, M.; Herbert, J.-M.; Fava, R.; Matthys, P.; Carmeliet, G.; Collen, D.; Dvorak, H. F.; Hicklin, D. J.; Carmeliet, P. *Nat. Med.* **2002**, *8*, 831−840.
(39) Deonarine, K.; Panelli, M. C.; Stashower, M. E.; Jin, P.; Smith, K.; Slade, H. B.; Norwood, C.; Wang, E.; Marincola, F. M.; Stroncek, D. F. *J. Transl. Med.* **2007**, *5*, 11.
(40) Gillitzer, R.; Goebeler, M. *J. Leukocyte Biol.* **2001**, *69*, 513−521.
(41) Scott, R. C.; Rosano, J. M.; Ivanov, Z.; Wang, B.; Chong, P. L.-G.; Issekutz, A. C.; Crabbe, D. L.; Kiani, M. F. *FASEB J.* **2009**, *23*, 3361−3367.
(42) Li, F.; Sun, J.-Y.; Wang, J.-Y.; Du, S.-L.; Lu, W.-Y.; Liu, M.; Xie, C.; Shi, J.-Y. *J. Controlled Release* **2008**, *131*, 77−82.
(43) Alemdaroğlu, C.; Degim, Z.; Celebi, N.; Sengezer, M.; Alömeroglu, M.; Nacar, A. *J. Biomed. Mater. Res., Part A* **2008**, *85*, 271−283.
(44) Meyer, J.; Whitcomb, L.; Collins, D. *Biochem. Biophys. Res. Commun.* **1994**, *199*, 433−438.
(45) Colletier, J.-P.; Chaize, B.; Winterhalter, M.; Fournier, D. *BMC Biotechnol.* **2002**, *2*, 9.
(46) Sou, K.; Naito, Y.; Endo, T.; Takeoka, S.; Tsuchida, E. *Biotechnol. Prog.* **2003**, *19*, 1547−1552.
(47) Korsmeyer, R. W.; Gurny, R.; Doelker, E.; Buri, P.; Peppas, N. A. *Int. J. Pharm.* **1983**, *15*, 25−35.
(48) Huang, X.; Brazel, C. S. *J. Controlled Release* **2001**, *73*, 121−136.
(49) D'Souza, S. S.; Faraj, J. A.; DeLuca, P. P. *AAPS PharmSciTech* **2005**, *6*, E553−64.
(50) Costa, P.; Sousa Lobo, J. M. *Eur. J. Pharm. Sci.* **2001**, *13*, 123−133.
(51) Dash, S.; Murthy, P. N.; Nath, L.; Chowdhury, P. *Acta Polym. Pharm.* **2010**, *67*, 217−223.
(52) Sessa, G.; Weissmann, G. *J. Lipid Res.* **1968**, *9*, 310−318.
(53) Shinitzky, M.; Inbar, M. *Biochim. Biophys. Acta, Biomembr.* **1976**, *433*, 133−149.
(54) Scott, R. C.; Rosano, J. M.; Ivanov, Z.; Wang, B.; Chong, P. L.-G.; Issekutz, A. C.; Crabbe, D. L.; Kiani, M. F. *FASEB J.* **2009**, *23*, 3361−3367.
(55) Carraway, K. L.; Cerione, R. A. *Biochemistry* **1993**, *32*, 12039−12045.
(56) Brandl, F.; Hammer, N.; Blunk, T.; Tessmar, J.; Goepferich, A. *Biomacromolecules* **2010**, *11*, 496−504.